

Paper ID ICLASS06-225

THE EFFECTS OF TEMPERATURE AND PRESSURE CHANGES ON SPRAY PROPAGATION AT CONSTANT AIR DENSITY IN AN INJECTION CHAMBER

Koch ¹ and Leipertz ²

¹ Ph.D. student, Dept. of Technical Thermodynamics (LTT), University of Erlangen-Nuremberg, pk@litt.uni-erlangen.de

² Professor, Dept. of Technical Thermodynamics (LTT), University of Erlangen-Nuremberg, sek@litt.uni-erlangen.de

ABSTRACT The injection system is one of the key components of direct injection combustion engines. Its characterization inside the engine is, due to the restrictions concerning the optical accessibility and the coupled interaction from several parameters of and on the injection process, difficult. A remedy is given by the use of optical injection chambers to investigate the spray propagation and evaporation at defined conditions, detached from the influences of e.g. the velocity field and the combustion chamber walls. These pressure vessels are able to work at engine relevant conditions concerning pressure and temperature. In this paper the influence of different chamber pressures and temperatures on the spray propagation for a constant chamber air density was investigated by the use of the Mie scattering light.

Keywords: Optical Diagnostic, High Pressure High Temperature Injection Chamber, Diesel Spray

1. INTRODUCTION

Due to the increasing political and public awareness for environmental concerns the reduction of the fuel consumption and the exhaust gas emissions are the two main interests for modern direct injecting diesel engines. There are more different possibilities to achieve these goals, whereas the injection system constitutes the main component of all these possible solutions. Hence, for the development of DI engines the precise adaptation of the injection process to the further mixture formation and combustion process is of central importance. The characteristics of the injected fuel spray directly influences all succeeding parts of the functioning chain. Especially the high pressure fuel injection and the variable injection timing by the use of modern injectors in combination with common-rail systems showed very promising results. Due to the higher spray momentum and the generation of smaller droplets the processes of evaporation and mixture formation are significantly improved. Because of the different interacting processes inside the combustion chamber an extensive characterization of the liquid fuel phase inside the engine is very difficult. The swirl motion of the intake air as well as the quickly changing ambient conditions are only two effects complicating the measurements. To be independent from these external influences and in order to concentrate on the liquid phase behavior itself injection chambers are particularly suitable. As examination methods laser measurement techniques are capable tools for such spray investigations, as they offer a high temporal and spatial resolution and are non-intrusive. For this investigation a continuously streamed high pressure high temperature injection chamber was used to determine the pressure and temperature influence on the spray propagation at one constant chamber air density. For the visualization of the liquid fuel propagation and distribution the Mie Scattering light technique was used. In this way, the determination of several spray parameters like for example tip penetration length and cone angle was determined. The results of the optical investigation as well as the subsequent data

evaluation show the importance of the pressure and temperature on the spray propagation at one identical chamber density. [1]

2. EXPERIMENTAL SET-UP AND MEASURING TECHNIQUES

2.1 High Pressure High Temperature Injection Chamber
The experiments have been performed inside a high pressure high temperature injection chamber (HPHT). The characteristic data of the utilized measuring object is summarized in

Table 1.

Table 1: Injection Chamber

maximum pressure	55 bar relative
maximum temperature	823 K
maximum air flow rate	65 m ³ /h
clearance of the optical accesses	120 mm
medium	nitrogen or air
volume	6 liter

The chamber is heated by a stationary air flow, whereas the velocity of the air flow inside the investigated spray region is less than 0.1 m/s. The adjustable range for investigations in the injection chamber is from 20 up to 550 °C and from 0 up to 55 bar overpressure concerning temperature and pressure values. The chamber pressure can be adjusted independently from the temperature. Looking at the maximum pressure and temperature values of the HPHT injection chamber in

Table 1, it becomes obvious that engine like density conditions for partial load operation modes are practicable. As basis for the density variation an operating point of the partial load region at the start of injection was chosen. With a pressure of 45 bar and a temperature of 778 K an approximate air density of 20 kg/m³ was adjusted. The conditions for the two other investigated points will be

described in a more detailed form later at the sub-item operating points. [2]

2.2 Injection System

The key elements of the injection apparatus are the first generation common rail system and the solenoid injector. The high pressure system is designed for a maximum pressure of 1350 bar. The pump of the engine fuel supply is powered by an electrical actuator and can thus be easily adjusted to the desired settings. For the investigations a mini sac-hole-nozzle with six holes was used. The nozzle has a rated flow of $Q_{hyd} = 360 \text{ cm}^3/30 \text{ s}$ at 101/1 bar, a spray angle of 160° and shows no slop angle. The nozzle details are listed in

Table 2.

Table 2: Nozzle Data

Notation	flow coefficient μ [-]	hole shape k_s [-]	nominal orifice diameter [mm]	HG hydro-grinding [%]
DLLA 908	0,86	1,5	0,137	10,5

The first generation common rail injection system together with the nozzle and the injector has been supplied by the Robert Bosch GmbH. For the researched operating points a reference diesel from Haltermann (RF-06-03) was used. As injection control unit a Genotec activation was applied, which allows a flexible configuration of the injection process.

2.3 Optical Diagnostics

For the investigation of the spray behaviour the well known Mie scattering light technique has been adjusted to this particular measurement problem. This technique is based on the elastic scattering of light at phase interfaces and can be used to detect the liquid fuel phase. The acquisition of the spray propagation behaviour was achieved via flash lamp illumination. In Figure 1 the optical set-up for the measurements is depicted. [3]

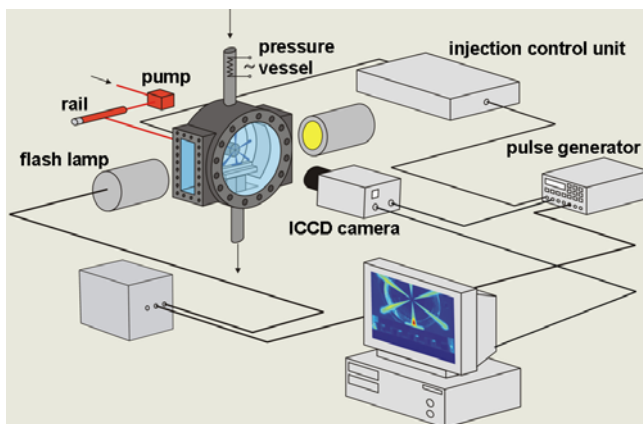


Figure 1: Measurement Set-up

The injection control unit, the flash lamps, the 12 bit intensified CCD camera and the readout computer are

connected and timed by a pulse generator. The detection of the spray signals occur perpendicular to the inserted illumination with an ICCD camera. The exposure time was 300 ns and 30 single shot images were recorded in steps of $100 \mu\text{s}$ starting from the visible start of injection and ending $2000 \mu\text{s}$. From the optical data average and standard deviation images were calculated. The post-image processing of the optical results for the derivation of important spray data like cone angle and penetration depth was conducted with the program SplashD. The nozzle was assembled under an angle in order to correct spray angle of 160° . In this way the spray cone entering the pressure chamber at 6 o'clock propagates straightforward during the whole injection process. Thus no corrections have to be conducted for the evaluation of the spray data for this fuel jet. The spray characteristics shown later in this contribution are calculated only for this spray cone and set to be representative for the other 5.

3. OPERATING POINTS

The object of these measurements was the investigation of the spray propagation for a variation of pressure and temperature at one constant chamber air density. The total amount of injected fuel for all three operating points was 55 mg at a rail pressure of 800 bar. The alteration of the caloric variables of state result in the matrix of the operating points shown in

Table 3.

Table 3: Matrix of Operating Points

operating point	p [bar]	T [K]	ρ_{air} [kg/m ³]
1	17,8	308	20
2	30,3	523	20
3	45,0	778	20

4. RESULTS AND DISCUSSION

4.1 Operating Point 1 (OP1)

Figure 2 shows a sequence of four averaged images taken in intervals of $400 \mu\text{s}$ after the visible start of injection for the operating point at ambient temperature conditions.

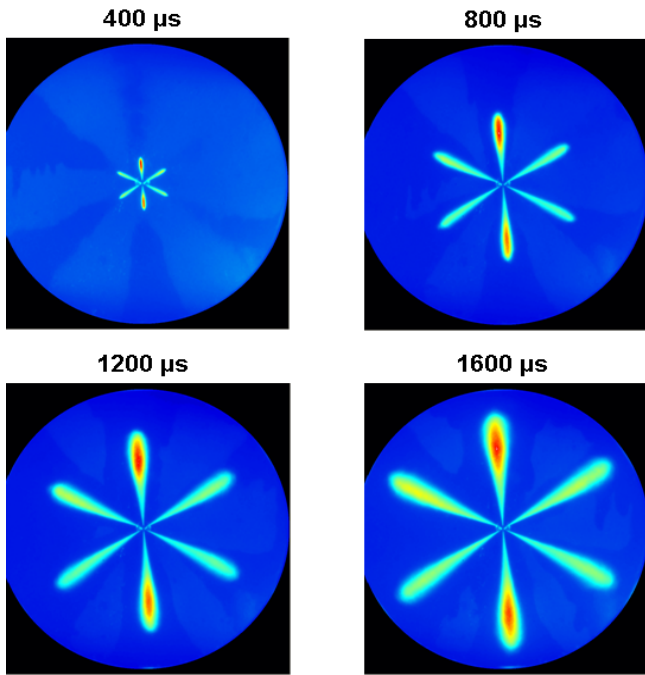


Figure 2: Sequence OP1

The increase of the signal intensity is demonstrated by the use of a color variation from blue over green, yellow to red. Due to the illumination from two sides and thus the superposition of the inserted light, the spray cones propagating in the center show higher signal intensities. The structure visible on the background of the images results from a moistening of the back plate, as the pressure and temperature level of this operating is not sufficiently high enough to evaporate the amount of injected fuel totally. The sequence of OP1 shows over the entire spray propagation process a development of rather wide spray cones, which exceed the dimension of the optical access at about 2000 μ s. For all operating point this moment represents also the last observation point being evaluated for the calculation of the spray cone angle and the penetration depth. The beginning of the evaluation was set at 400 μ s after visible start of injection in order to circumvent the deviation caused by the nozzle. In Figure 3 the contour plot and the appearance probability including the time steps until 2000 μ s after the visible SOI for OP1 is depicted.

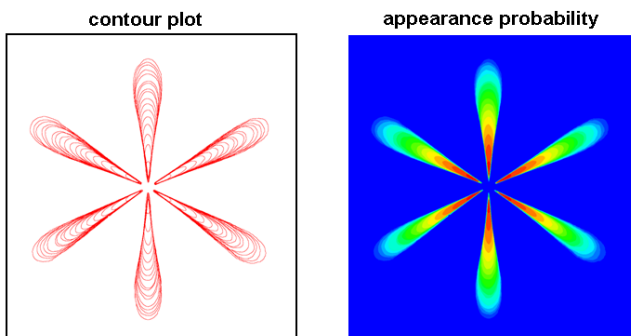


Figure 3: Contour Plot and Appearance Probability OP1

The contour plot shows a uniform propagation of the fuel with nearly equally spaced steps between the observation points. The coloring of the appearance probability image has a similar meaning like mentioned before. Blue denotes the lowest and red the highest probability of fuel appearance at

the particular location. Nearly a hundred per cent probability of fuel appearance is given for a range of 30 % of the total spray penetration. With spray propagation the probability decreases in direction of the spray tip.

4.2 Operating Point 2 (OP2)

For this operating point the pressure and temperature settings were increased to a level lying between the two extremes:

- OP1 ambient temperature condition
- OP3 partial load real engine behaviour

One of the main advantages of the pressure and especially the temperature increase consists of the fact that the moistening of the background is strongly decreased due to the enforced evaporation of the fuel. Therefore distracting structures and reflections from the background are inhibited. In Figure 4 the sequence for this operating point is depicted. The time steps are chosen in equal intervals according to OP1. The background of these images appears darker than the one of the previous measuring point as the false-color representation is adjusted to each moment and operating point separately. For all signals a min.-max. color adjustment was chosen to achieve the maximum amount of information from all spray images. With regard to the spray appearance at 400 μ s after the visible start of injection no significant difference is detectable. At 800 μ s the deviations are much more obvious, the penetration depth is shorter and the spray body more compact. The main reason for these effects results from the increased chamber pressure and thus the enhanced resistance acting against the spray propagation. The next two time steps show a similar behaviour, whereas the region of high signal intensity is locally more concentrated towards the spray tip and the intermediate range is less distinctive.

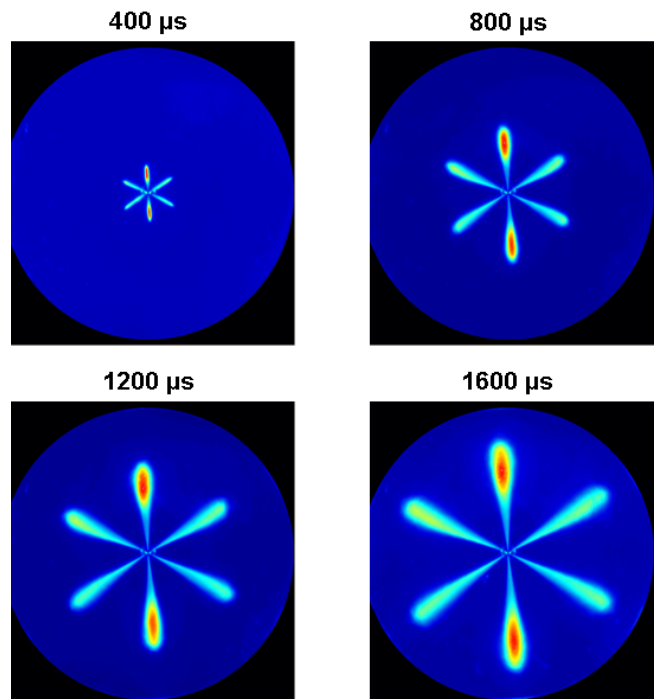


Figure 4: Sequence OP2

In Figure 5 the contour plot and the appearance probability until 2000 μ s after SOI is shown. The conclusions resulting

from the averaged images in Figure 4 become reinforced and more obvious by the contour plot.

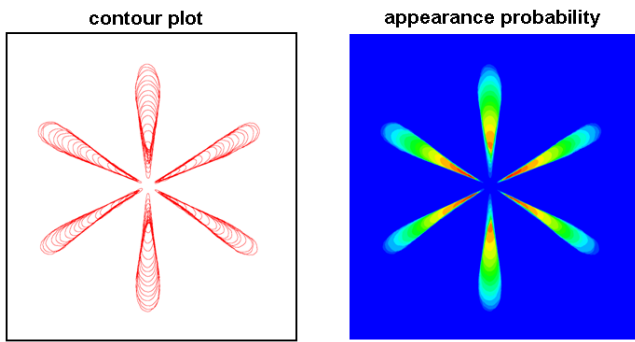


Figure 5: Contour Plot and Appearance Probability OP2

The most apparent difference to OP1 is the deformation of the spray tip, where a sharper structuring of the side area appears. Besides this a movement of the entire spray body away from the nozzle is considerable. This effect can also be seen in appearance probability image. Due to this shift, regions with almost a hundred per cent fuel probability no longer appear. Moreover the decrease of signal at the spray tip shows a more structured decay.

4.3 Operating Point 3 (OP3)

OP3 represents the starting point for the calculations of the HPHT injection chamber density. The temperature and pressure values of this operating point were chosen as they are representative for real engine working conditions in a partial load range. Figure 6 shows the sequence of the optical analysis conducted for this measuring point.

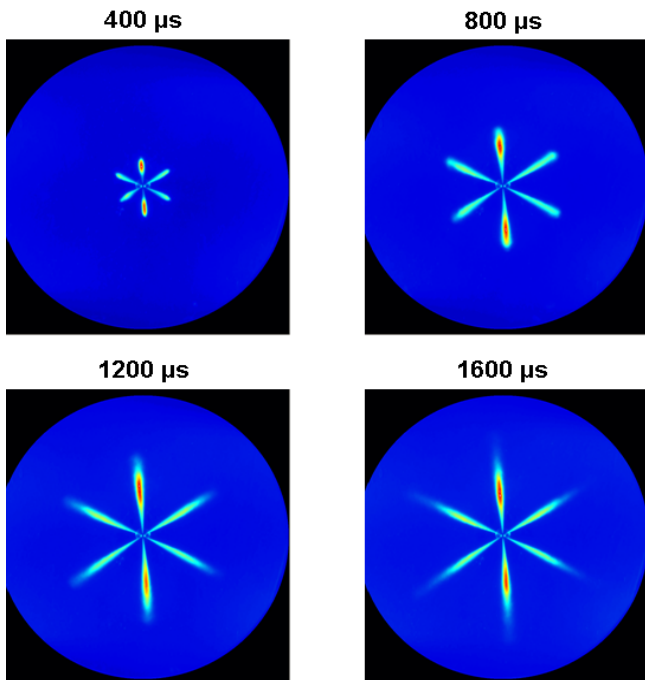


Figure 6: Sequence OP3

During the time period briefly after the start of injection no significant differences from the spray behaviour of OP1 and OP2 are detectable. At 800 μs after the SOI a noticeable decrease in the spray penetration depth and the shaping of

the spray body becomes apparent. Especially the width of the spray cone is getting smaller. With increasing observation time the differences in comparison to the operating points discussed before become even more obvious. Whereas the operating points 1 and 2 show within the time range of 1200 μs until 1600 μs significant changes concerning the spray propagation, nearly no alteration for this OP becomes visible. Moreover no decisive modification of the spray body within this period occurs. The influence of starting combustion processes at this temperature and pressure level can be neglected, as only moments up to 2000 μs after SOI are considered and first important ignition reaction are starting afterwards. All these differences appear in the contour plot and appearance probability in Figure 7 too.

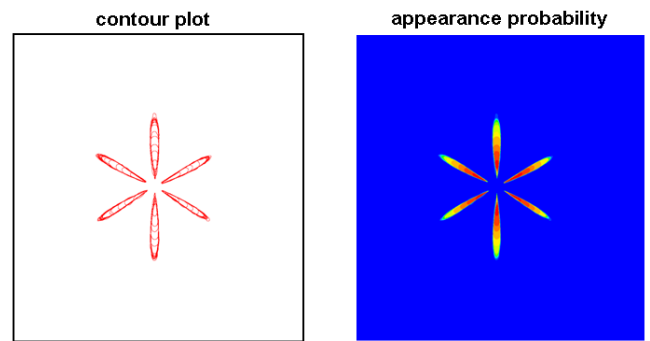


Figure 7: Contour Plot and Appearance Probability OP3

The contour plot shows a highly uniform and nearly equally spaced fuel propagation over the whole observed period of time. Moreover the shaping of the spray cone is narrower and spray tip is less rounded. The image of the appearance probability shows a constant stepping within the decrease of fuel occurrence from the nozzle exit up to the spray tip.

4.4 Combined Results of the Data Evaluation

In the following paragraph the results of the image evaluation for all three operating points will be discussed in a comprehensive way. Therefore the results of the single operating point measurements are combined in single diagrams. In Figure 8 the developing of the penetration depth values with the time after SOI is depicted.

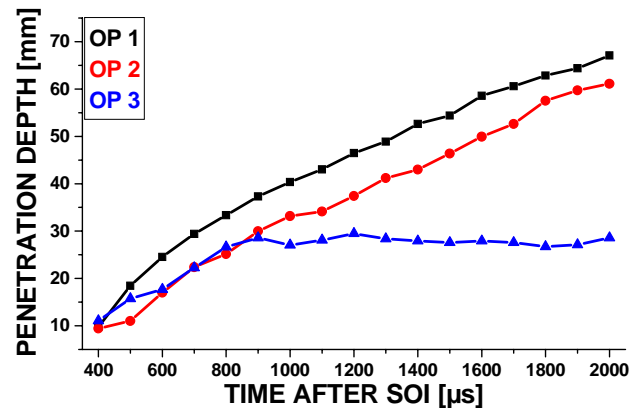


Figure 8: Developing of the Penetration Depth with Time

Except of the absolute numbers, the developing of the values

from OP1 and OP2 are very similar. The operating point with the lowest pressure and temperature level shows in this case the highest absolute values and also the most uniform developing of the graph. For OP3 900 μs after the SOI the spray penetration depth remains nearly constant until the end of the observation. The maximum value is only one third of the one for OP1. Moreover the fuel jet of OP1 reaches certain penetration depth values much faster.

The development of the spray area with time is displayed in Figure 9 on the following page.

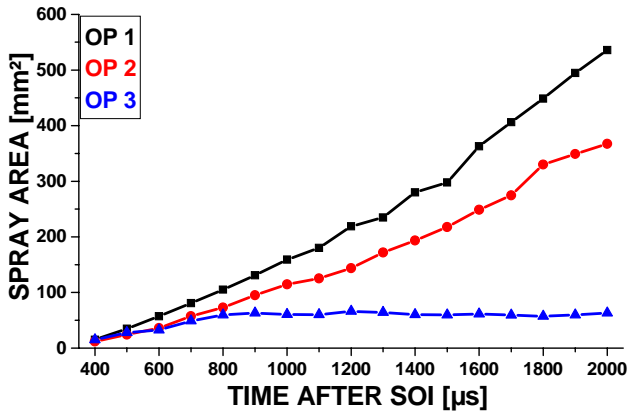


Figure 9: Developing of the Spray Area with Time

Besides the information already contained in Figure 8, this diagram gives additional conclusions about width of the spray body and its further forming. For the operating points 1 and 2 the diagram shows two strongly increasing straight lines which allow the conclusion that the propagation of the spray body is not only in the direction of the symmetry axis but also perpendicular to it. By contrast to this behaviour the spray area of OP3 keeps constant after 900 μs after SOI. In connection with the results of Figure 8, the operation point with the partial load engine conditions shows no more significant changes at the formation of the spray body after this point of time. Due to the stronger broadening of the spray body at lower pressure levels, the difference in absolute values becomes for this illustration even more noticeable.

Besides the two calculated dimension also an evaluation of the images regarding the spray cone angle was accomplished. The result of this calculation is displayed in Figure 10.

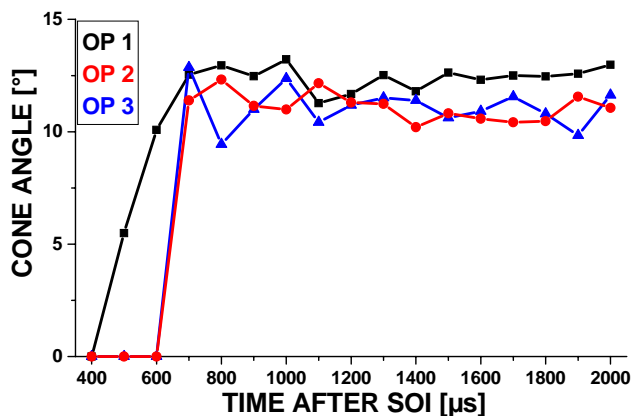


Figure 10: Developing of the Cone Angle with Time

The lack of data especially of the operating points 2 and 3 at early time steps results from the disturbance of the angle determination due to reflections of the nozzle. Over the whole observed time period no significant difference of the cone angle for all three operating points are detectable. This is unsurprising; as the density is the main influencing parameter on this value. The minimum differences within the three graphs are located within the deviations of the determination process.

6. CONCLUSION

In this study measurements were conducted inside a high pressure high temperature injection chamber with a stationary air flow in order to demonstrate the importance of pressure and temperature at one constant chamber air density. To achieve this goal a simplified optical set-up with two flash lamps for the generation of the Mie scattering was used. The initial value of the density was determined under the condition of real engine load achievable with the existing mechanical requisites. Starting from this value two other pressure and temperature settings were chosen, one at ambient conditions and one between the two boundary values. The spray propagation process was observed from the start of injection until the end of visibility of liquid fuel phase. For the evaluation of the optical data only the timeframe beginning with the visible start of injection and ending with starting of combustion at the operation point with the highest load.

The operating point with the lowest pressure and temperature level shows the largest values for the penetration depth and the spray area. Moreover certain penetration depths are also attained much faster. Also the broadening of the spray body is the strongest for this operating point. The investigated point with medium conditions shows a similar behaviour to operating point 1 but less distinctive. For the measurements at engine-like conditions in the partial load range 900 μs after the SOI a stagnation of the penetration depth occurs. Besides this also a further formation of the spray cone stops. An influence of the pressure and temperature level on the spray angle could not be detected. As a conclusion it can be said that, due to a higher resistance and increased evaporation the chamber pressure and temperature at a constant density shows a distinct effect on the spray propagation. Thus, not only the density can be used to characterize an engine operation point completely.

7. DEFINITIONS

CR	common rail	[-]
DI	direct injection	[-]
DLLA	mini sac-hole-nozzle	[-]
HG	hydro grinding	[-]
HPHT	high pressure high temperature	[-]
ICCD	intensified charge coupled device	[-]
k	k-factor, conical nozzle shape	[-]
Mie	Mie scattering technique	[-]
OP	operating point	[-]
p	pressure	[bar]
Q_{hyd}	rated hydraulic flow	[cm ³ /30s]
RF	reference fuel	[-]

SOI	start of injection	[-]
s	cavitation free nozzle hole	[-]
T	temperature	[K]
ρ	density	[kg/m ³]
μ	flow coefficient	[-]

8. REFERENCES

- [1] Ipp, W., Lindner, R., Goldlücke, J., Lutz, M., Schmitz, I., Leipertz, A., Injection Chamber Test Rigs for the Optical Investigation of Diesel Nozzles at Engine Relevant Conditions, Proc. VII. Congress on Engine and Combustion Processes (HDT Munich 05), pp.223 -232, 2005
- [2] Schünemann, E., Experimentelle Untersuchungen zur Interaktion zwischen Einspritzstrahl und Brennraumwand bei der dieselmotorischen Gemischbildung, Ph.D. thesis, Lehrstuhl für Technische Thermodynamik, 1999
- [3] Münch, K. U., Fath, A., Leipertz, A., Comparison between different visualization techniques for investigation of atomization processes in engines, Proc. Colloquium on the combustion of Drop, Sprays and Aerosols (EUROMECH 324 Marseille 94), 1994